



**HAL**  
open science

## **Gemini North Adaptive Optics (GNAO): an MCAO system for Gemini North towards Conceptual Design**

Gaetano Sivo, David Palmer, Julia Scharwächter, Morten Andersen, Natalie Provost, Eduardo Marin, Marcos van Dam, Brian Chinn, Emmanuel Chirre, Charles Cavedoni, et al.

► **To cite this version:**

Gaetano Sivo, David Palmer, Julia Scharwächter, Morten Andersen, Natalie Provost, et al.. Gemini North Adaptive Optics (GNAO): an MCAO system for Gemini North towards Conceptual Design. 6th International Conference on Adaptive Optics for Extremely Large Telescopes, AO4ELT 2019, Jun 2019, Quebec City, Canada. hal-02862325

**HAL Id: hal-02862325**

**<https://hal.science/hal-02862325v1>**

Submitted on 9 Jun 2020

**HAL** is a multi-disciplinary open access archive for the deposit and dissemination of scientific research documents, whether they are published or not. The documents may come from teaching and research institutions in France or abroad, or from public or private research centers.

L'archive ouverte pluridisciplinaire **HAL**, est destinée au dépôt et à la diffusion de documents scientifiques de niveau recherche, publiés ou non, émanant des établissements d'enseignement et de recherche français ou étrangers, des laboratoires publics ou privés.

# Gemini North Adaptive Optics (GNAO): an MCAO system for Gemini North towards Conceptual Design

Gaetano Sivo<sup>a</sup>, David Palmer<sup>b</sup>, Julia Scharwächter<sup>b</sup>, Morten Andersen<sup>a</sup>, Natalie Provost<sup>a</sup>, Eduardo Marin<sup>a</sup>, Marcos van Dam<sup>c</sup>, Brian Chinn<sup>a</sup>, Emmanuel Chirre<sup>a</sup>, Charles Cavedoni<sup>b</sup>, Thomas Schneider<sup>b</sup>, Stacy Kang<sup>b</sup>, Paul Hirst<sup>b</sup>, William Rambold<sup>b</sup>, Angelic Ebberts<sup>b</sup>, Pedro Gigoux<sup>a</sup>, Laure Catala<sup>b</sup>, Thomas Hayward<sup>a</sup>, John Blakeslee<sup>a</sup>, Henry Roe<sup>a</sup>, Jennifer Lotz<sup>d</sup>, Scot Kleinman<sup>b</sup>, Manuel Lazo<sup>a</sup>, Celia Blain<sup>b</sup>, Suresh Sivanandam<sup>e</sup>, Anja Feldmeier-Krause<sup>f</sup>, Mark Ammons<sup>g</sup>, Chadwick Trujillo<sup>h</sup>, Chris Packham<sup>i</sup>, Franck Marchis<sup>j</sup>, Julian Christou<sup>k</sup>, James Jee<sup>l</sup>, John Bally<sup>m</sup>, Mike Pierce<sup>n</sup>, Thomas Puzia<sup>o</sup>, Paolo Turri<sup>p</sup>, Hwi Hyun Kim<sup>a</sup>, Meg Schwamb<sup>b</sup>, Trent Dupuy<sup>b</sup>, Ruben Diaz<sup>a</sup>, Rodrigo Carrasco<sup>a</sup>, Benoit Neichel<sup>q</sup>, Carlos Correia<sup>r</sup>, Eric Steinbring<sup>s</sup>, François Rigaut<sup>t</sup>, Jean-Pierre Véran<sup>s</sup>, Mark Chun<sup>u</sup>, Masen Lamb<sup>e</sup>, Scott Chapman<sup>v</sup>, Simone Esposito<sup>w</sup>, and Thierry Fusco<sup>x,q</sup>

<sup>a</sup>Gemini South Observatory, La Serena, Chile

<sup>b</sup>Gemini North Observatory, Hilo, United States of America

<sup>c</sup>Flat Wavefront, Christchurch, New Zealand

<sup>d</sup>Gemini Observatory, Tucson, United States of America

<sup>e</sup>University of Toronto, Toronto, Canada

<sup>f</sup>University of Chicago, Chicago, United States of America

<sup>g</sup>Lawrence Livermore National Lab, Livermore, United States of America

<sup>h</sup>Northern Arizona University, Flagstaff, United States of America

<sup>i</sup>University of Texas San Antonio, San Antonio, United States of America

<sup>j</sup>Search of ExtraTerrestrial Intelligence, Mountain View, United States of America

<sup>k</sup>Large Binocular Telescope Observatory, Tucson, United States of America

<sup>l</sup>Yonsei University, Seoul, South Korea

<sup>m</sup>University of Colorado, Boulder, United States of America

<sup>n</sup>University of Wyoming, Laramie, United States of America

<sup>o</sup>Pontificia Universidad Católica, Santiago, Chile

<sup>p</sup>University of California Berkeley, Berkeley, United States of America

<sup>q</sup>Laboratoire d'Astrophysique de Marseille, Marseille, France

<sup>r</sup>Keck Observatory, Waimea, United States of America

<sup>s</sup>Herzberg Astronomy and Astrophysics, Victoria, Canada

<sup>t</sup>Australian National University, Canberra, Australia

<sup>u</sup>Institute for Astronomy, Hilo, United States of America

<sup>v</sup>Dalhousie University, Nova Scotia, Canada

<sup>w</sup>Osservatorio Astronomico di Arcetri, Florence, Italy

<sup>x</sup>Office national d'études et de recherches aérospatiales, Châtillon, France

## ABSTRACT

Gemini Observatory has been awarded from the National Science Foundation a major fund to build a new state-of-the-art Multi Conjugate Adaptive Optics facility for Gemini North on Maunakea called GNAO. The current

---

Further author information: (Send correspondence to Gaetano Sivo)

Gaetano Sivo: E-mail: gsivo@gemini.edu, Telephone: 1+56 51 2205 642

baseline system will use two lasers each split in two to create an artificial constellation of four laser guide star to measure the distortions caused by the atmosphere. At least two deformable mirror conjugated to 0km and the main altitude layer above Maunakea will be used to correct these distortions. The facility will be designed to feed future instrumentation, initially a near infrared imager and potentially a visiting 4-arm multi object adaptive optics IFU spectrograph.<sup>1</sup> In this paper I will present the main characteristics of this exciting facility, its promises and its challenges. I will also present its conceptual design and results of trade studies conducted within the team and the Gemini Adaptive Optics Working Group. The expected first light is for October 2024.

**Keywords:** Adaptive Optics, Multi-conjugate adaptive optics, GeMS, GNAO, High Angular Resolution, Gemini Observatory

## 1. INTRODUCTION

Gemini Observatory has been awarded a major founding from the National Science Foundation to build a full new state of the art multi-conjugate adaptive optics system for Gemini North. The objective of this award is to enable rapid response and high angular resolution observations in the era of multi-messenger astronomy.<sup>2</sup> Gemini together with the Gemini North Adaptive Optics (GNAO) science team have developed a list of key science cases that will drive the definition of the top level requirements of the AO system in order to answer the observations of these targets. The requirements for GNAO are driven by a broad range of science cases which will greatly benefit from extending Geminis MCAO coverage into the Northern hemisphere. As a unique high-angular-resolution facility for multi-messenger astronomy, transient follow-up, and other time domain work, GNAO is further designed to maximize synergy with the two major upcoming astronomical facilities, the Large Synoptic Survey Telescope (LSST) and the James Webb Space Telescope (JWST). Requirements from the science cases are important drivers for the GNAO/RTC design. Some of the crucial parameters are the spectral range, field-of-view, Strehl ratio, PSF uniformity as well as PSF temporal/spatial stability, astrometric accuracy, and sky coverage. In addition, the science cases and concept of operations define a number of operational requirements which include non-sidereal tracking, availability on a nightly basis, and a choice of narrow-field versus wide-field optimized AO correction.

The main requirements for this system are:

- to deliver a close to diffraction limit in the near infrared on a 2 arc minutes field of view;
- obtain a correction of 30% Strehl ratio in K-band with a goal of 50%;
- obtain a precision astrometry of 0.2 mas across the field (goal of 0.1mas);
- operate under 1.2" seeing conditions at 0.5um or better (goal 1.5");
- deliver an output science beam at f/32;
- sky coverage of 20% at the galactic pole with 3 natural guide stars (goal of 30%) and 60% with one natural guide star (goal 75%);
- operable in queue mode with no more than the standard telescope operator + science observer manpower;
- be modular to enable future very wide field ground layer AO mode.

## 2. OVERALL ARCHITECTURE AND SUBSYSTEM DESCRIPTION

The Gemini North Adaptive Optics (GNAO) system is a multi-conjugate AO (MCAO) system for Gemini North like GeMS at Gemini South.<sup>3,4</sup> GNAO is a next generation MCAO system designed for a wide range of science cases. The aim is to produce near diffraction-limited image quality for J-, H- and K-bands. The requirement is for stable image quality across a 2 diameter field, with a K-band Strehl of between 0.3 (requirement) and 0.5 (goal) under median seeing conditions and nominal 3-NGS constellation. The system would use 2 deformable mirrors (DMs) at first light at conjugate altitudes of 0 km and 11.4 km. When an adaptive secondary mirror (ASM) is added, the DM conjugated to the ground can be moved to a conjugate altitude of 4 km. LGS-based AO systems

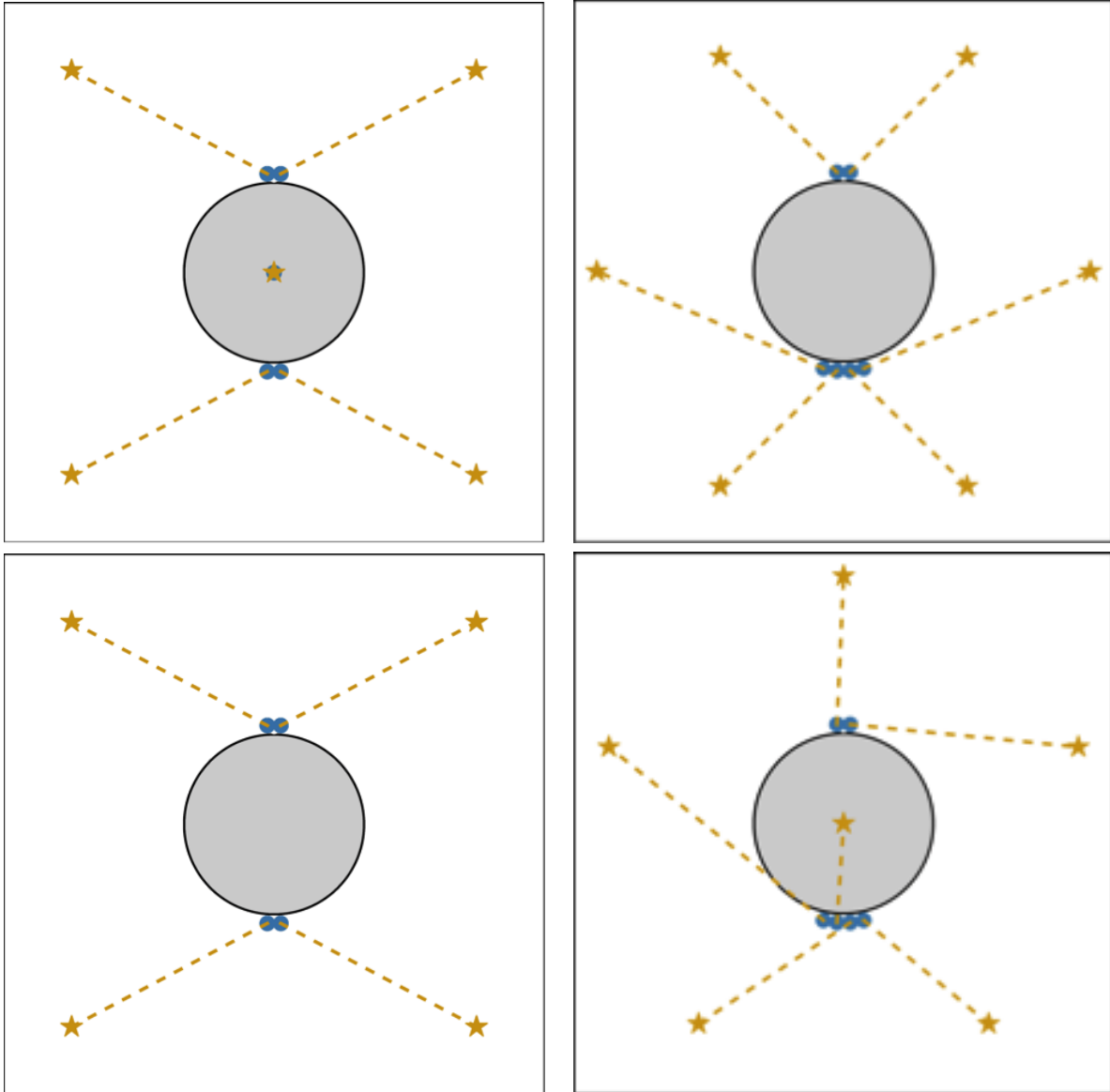


Table 1. Bottom left: LGS Constellation on-sky Configured by 2 Lasers, 4 Stars, 4 Launch Telescopes referred hereafter as Configuration 3. Top left: LGS Constellation on-sky Configured by 3 Lasers, 5 Stars, 5 Launch Telescopes referred hereafter as Configuration 1. Top right: LGS Constellation on-sky Configured by 3 Lasers, 6 Stars, 6 Launch Telescopes referred hereafter as Configuration 2. Bottom right: LGS Constellation on-sky Configured by 3 Lasers, 6 Stars, 5 Launch Telescopes with 1 center launched referred hereafter as Configuration 4.

require natural guide stars (NGSs) to measure tip-tilt and focus. GNAO has a sky coverage requirement at the galactic pole of 60% when using a single NGS, and 20% when using three NGSs. GNAO will use a constellation of 4 laser guide star at first light on a square with a path to bring a fifth star at the center of the field later on. The laser guide star facility is described in section ???. The LGS constellation on-sky will be of 4 stars in a square of 50 in diameter coming out of 2 Toptica lasers each split in 2 and feeding their own independent side launch laser telescope. The table 1 shows the different constellations considered.

The adaptive optics bench called AOS will be designed with 5 laser guide star wavefront sensors (LGSWFSs) in order to have the 4 corners LGS fed and the possibility to answer some science cases requirements that do not intend to use the full field of view but rather high performance on-axis science. One of the laser spot will

Terms	Order	WFE(nm)
Scintillation	LGS	18
Dome seeing	LGS	39
M1 error Figure	LGS	32
M2 print-through	LGS	147
Atmospheric temporal bandwidth	LGS	50
LGS WFS measurement noise	LGS	43
Fratricide effect	LGS	21
Tomographic error	LGS	170
Generalized fitting error	LGS	204
LGS focus	NGS	30
TT atmospheric temporal bandwidth	NGS	25
TT telescope temporal bandwidth	NGS	234
TT noise	NGS	0
TT tomography (3NGS, typical)	NGS	172
Total	N/L GS	431
Goal (30% in K)		384

Table 2. Bright guide star wavefront error budget

be steered onto the center of the field to feed this on-axis WFS. The idea is also to have everything ready in the AOS subsystem for a future upgrade path that would consist to add a third laser to the LGSF and feed the central LGSWFS to have a full 5 LGS constellation system as presented in the right figure of table 1. The way to send the light from one corner star to the center is presented in Section ??.

The NGS WFS will be a focal plane WFS using a fast readout detector. The system will be able to use from 1 up to 3 NGS(s). The AOS subsystem will be designed to provide science light of 850nm and higher to the science instruments.

### 3. WAVEFRONT ERROR BUDGET

In this section, we present the error budget for the case where we are observing at zenith in median atmospheric conditions using a typical NGS asterism. All three NGS stars are assumed to be very bright (since there is no typical brightness). We separate the terms into LGS based terms (high-order modes) and NGS-based terms (tip-tilt, tip-tilt anisoplanatism, and focus due to sodium altitude variations). Only the dominant error budget terms are included.

The wavefront errors in an error budget are traditionally added in quadrature. This is a good approximation for single conjugate AO systems, but not as accurate for MCAO, where the error terms interact. In particular, wavefront sensing errors and wavefront correction errors can be double counted. Hence, the true wavefront error is lower than a sum in quadrature would predict.

The wavefront error is used to predict the Strehl ratio using the Marechal approximation. For Strehl ratios lower than about 60%, the Strehl ratio is higher than the Marechal approximation predicts.

#### 3.1 Scintillation

Scintillation results from high altitude wavefront aberrations propagating to the ground. If the wavefront is not corrected, the scintillation leads to a reduction in Strehl ratio that is equivalent to an additional wavefront error of 18 nm. This is reduced if the high-altitude turbulence is corrected by placing the DMs in the correct order (*i.e.*, ground-layer DM first), but increased if the order of the DMs is reversed (like on GeMS).

#### 3.2 Dome Seeing

The dome seeing is a measure of local turbulence within the dome and in the sheer layer flowing over the dome opening. The dome seeing optical path difference map corresponds to a low spatial frequency WF aberration. The dome seeing at Gemini is believed to be 0.13 at a wavelength of 500 nm. Assuming Kolmogorov statistics, simulations show that dome seeing leads to an additional residual wavefront of 39 nm.

### 3.3 M1 figure error

The numbers provided have been taken from the M1 acceptance review. A report is available to provide if needed.

### 3.4 M2 print-through

The secondary mirror at Gemini has a well-known print through error. The secondary mirror of the Gemini telescope is held on its back surface in three points, with an additional three mounting points for a safety system. Unfortunately, this structure has a print-through onto the optical surface; this high spatial frequency pattern has a detrimental effect on AO systems by introducing erroneous centroid offsets and additional noise (due to smeared spots at the focus of the lenslet array) on given sub-apertures. These artifacts are then fed back into the control loop as low spatial frequencies; the folding of high spatial frequencies onto low spatial frequencies is a typical case of aliasing. To first order, the amount of energy in a diffraction pattern is proportional to the area of the pupil generating the diffraction; therefore, the aliasing amplifies the deleterious effects of the print-through pattern as aliased low spatial frequencies cover a larger fraction of the pupil than the fairly localized pattern of the print-through. As the pupil rotates on the WFS to keep the field orientation constant on the detector, the centroid offsets due to the M2 print-through change continuously; it is therefore not sufficient to measure them once at fixed cass-rotator position angle since this does not allow to disentangle which part of the offsets is due to the print-through, and which is due to aberrations of other optics which may not rotate with respect to the pupil. This represents a major error term of this error budget breakdown. It is estimated to be 147 nm. This problem has been escalated to the GEMMA Executive Committee and a plan is in place to remediate this issue.

### 3.5 Atmospheric temporal bandwidth

The temporal bandwidth error, or also called servo-lag error, comes from the delay that exists in an AO loop in correcting the turbulence produced by the atmosphere. The bandwidth error increases with the evolution speed of the turbulence relative to the sampling of the loop. Increasing the frame rate reduces the bandwidth error. For GNAO running at 500Hz, this term is estimated to be 50 nm. The bandwidth error due to high-order wavefront errors induced by the telescope have not yet been considered.

### 3.6 LGS WFS measurement noise

The measurement noise comes from the photon noise (due to limited flux from the LGS), read noise of the detector, dark current and sky background. The excess noise inherent in the electron multiplication of an EM CCD is included in the simulations. The measurement noise can be reduced by reducing the frame rate or the loop gain. For GNAO, using laser guide stars and the current baseline presented in this document, we estimate it to be 43 nm.

### 3.7 Fratricide effect

The so-called fratricide effect is caused by the Rayleigh backscatter contaminating the signal from the sodium return. Contaminated sub-apertures are masked, since the measurement noise and bias in the centroids renders the measurements unusable. Discarding these measurements increases the wavefront error by 21 nm.

### 3.8 Tomographic reconstruction error

The tomographic error is the error due to lack of knowledge about the wavefront. This limitation results from the number and location of the laser guide stars as well as the sodium altitude. For a four LGS system, the error is 170 nm.

### 3.9 Generalized fitting error

The generalized fitting error is the error due to insufficient actuator density, both in the xy-plane (interactuator pitch) and along the z-direction (number of DMs). For a 2 DM system, this is the largest high-order wavefront error term (204 nm), and is largely independent of the conjugate altitude of the high-altitude DM. Adding more DMs decreases this error.

### 3.10 LGS focus error

We consider the focus errors due to sodium height variability. It is interesting to note that the sodium is not found outside of the altitude interval between 80 and 100 km above sea level. This is because sodium ionized above 100 km and reacts chemically with oxygen below 80 km. For a 7.9-m telescope, this implies that a 100-m error in sodium altitude estimation leads to 28 nm of wavefront error, and this is the level of accuracy that is required. We specify the allowable error to be 30 nm, and design the truth sensor accordingly.

### 3.11 TT atmospheric temporal bandwidth

The tip-tilt bandwidth error due to the atmosphere alone is small, since atmospheric tip-tilt changes slowly. Simulations indicate that this terms is of the order of 25 nm when running at 500 Hz.

### 3.12 TT telescope temporal bandwidth

The telescope and the cryostats in the science instruments introduce vibrations which dominate the wavefront error budget, even running at 1 kHz. It is likely that the error can be reduced from its current value of 234 nm by using more sophisticated controllers, at least for bright stars. This risk has also been escalated to the GEC. There is a clear path toward working on identifying the sources of these vibrations and the Observatory has a plan to mitigate them. An example of a TT spectra measured by ALTAIR (Gemini North classical AO system) is shown in the figure 1.

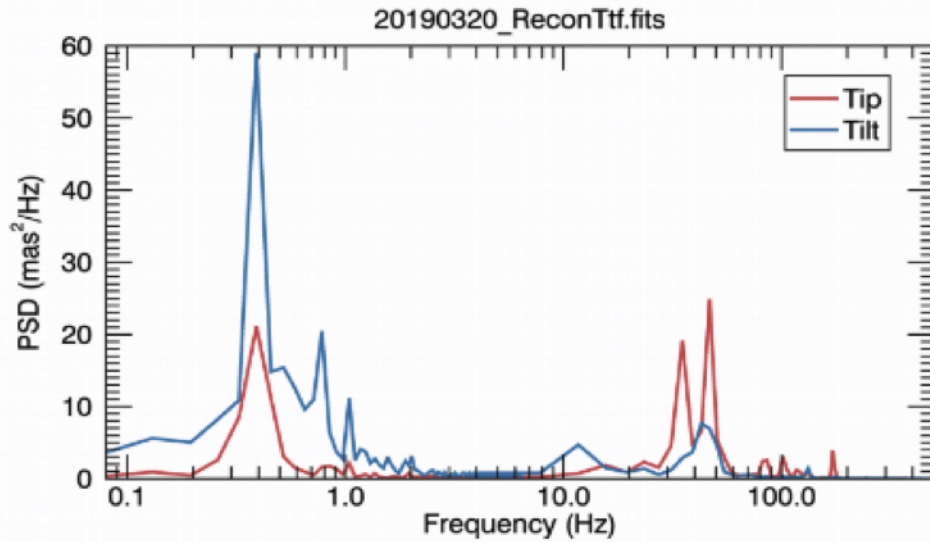


Figure 1. Power Spectral Density of the TT Disturbance Measured by ALTAIR

### 3.13 TT measurement noise

The tip-tilt measurement noise depends on the magnitude and location of the guide stars. This error has not been quantified for the different asterisms.

### 3.14 TT tomography

The number of tip-tilt guide stars used varies between one and three. The tip-tilt value at locations away from the tip-tilt stars is estimated using a tomographic reconstruction. For a typical 3-star asterism, the error in this estimate is 172 nm.

## 4. PERFORMANCE ASSESSMENT OF GNAO: SIMULATION STUDIES

We present in this section the simulations performed during the conceptual design phase and the different assumptions to understand the performance of our system. Parameter space is explored in order to see how the performance is impacted by the design.

## 4.1 Atmospheric Turbulence profiles

The atmospheric parameters are the 25th, 50th and 75th percentile sourced from the TMT study and courtesy shared to us (Table ??). The outer scale in every case is set to 30 m. Random wind directions were applied to the measured wind speeds. The design parameters will be optimized based on median seeing, and the performance evaluated for all three cases.

	Elevation (m)	0	500	1000	2000	4000	8000	16000
	Wind Speed (m/s)	5.6	5.77	6.25	7.57	13.31	19.06	12.14
	Wind Direction (°)	190	255	270	350	17	29	66
25%, $r_0 = 0.247\text{m}$	Turbulence fraction	0.5152	0.0951	0.0322	0.0262	0.1160	0.0737	0.1416
50%, $r_0 = 0.247\text{m}$	Turbulence fraction	0.4557	0.1295	0.0442	0.0506	0.1167	0.0926	0.1107
75%, $r_0 = 0.247\text{m}$	Turbulence fraction	0.3952	0.1665	0.0703	0.0773	0.0995	0.1069	0.0843

Table 3. Caption

## 4.2 Simulation parameters

The parameters used in the simulations are as follows:

- 16x16 SHWFS with 4x4 1" pixels
- the interactuato spacing of the DMs is the same as the pitch of the subapertures ( $\approx 50$ ) with one DM at 0km, the other at 14km
- three ideal TT stars for TT sensing to correct for TT and plate scale modes
- TT guide star locations (in arcsec) are [0,35]. [40,-30] and [-40,-20]
- simulations were run at zenith and 45 degrees elevations
- median atmospheric conditions
- including fratricide

## 4.3 Performance of GNAO

The average K-band Strehl ratio from the simulations is plotted in Figure 2, in conjunction with the standard deviation across the 2 diameter field in Figure 3. The results show that there is a soft dependence on radial distance, with the optimal average Strehl found for an LGS radial distance of 50 for Configuration 1, which also has an LGS at the center, and about 40 for the Configurations 2 and 3, which do not have the additional LGS. The variation in Strehl, however, decreases with increasing radial distance.

Figures in the Table 4 and Table 5 plots the variation in K-band Strehl ratio and FWHM across the field respectively. It is apparent that the best Strehl ratio is attained in the direction of the guide stars. For this reason, Configuration 1 produces the best on-axis Strehl ratio and should be preferred for narrow field science cases. The FWHM does not change significantly across the field.

We can see in these plots that the performance requirements are met in term of "pure" Strehl or FWHM for all the configurations. The same simulations were performed at 45 degrees and we came to the same conclusion. Another top level science requirement for GNAO is that the PSF should be stable both in time and spatially. Indeed, we want GNAO to produce a stable PSF across the field with a relative error of 10%. And we also want GNAO to produce a PSF that remains constant within 10% during two separated visit over a period less than 3 months. These requirements show that configuration 3 will be problematic to maintain the performance. Nevertheless, at the date of the conference, this is what was budgeted and was presented.



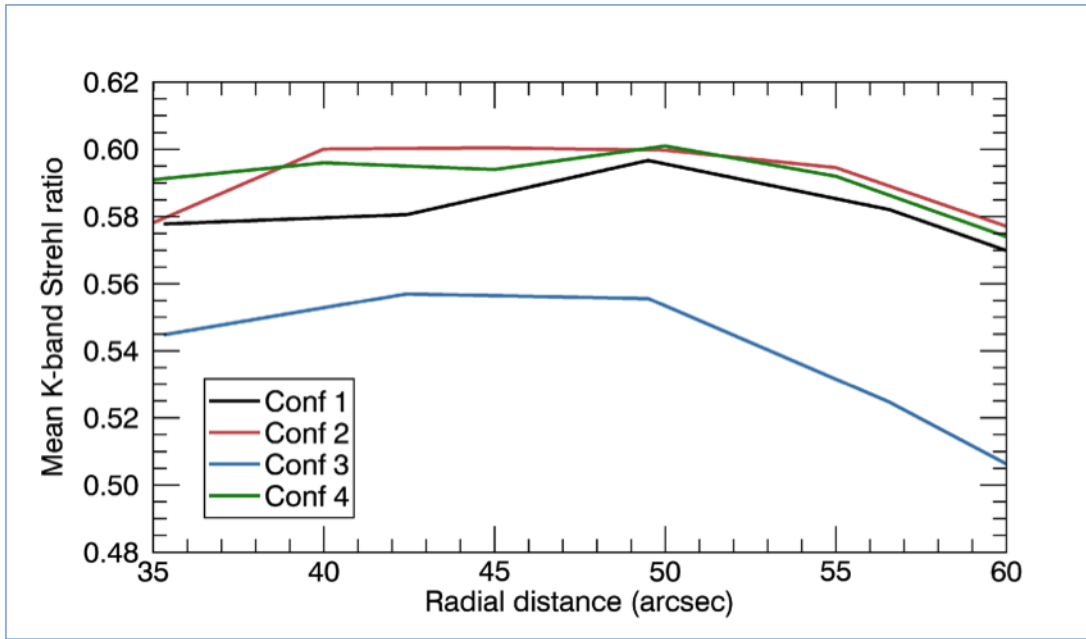


Figure 2. Simulated K-band Strehl ratio average for the three different configurations in median seeing

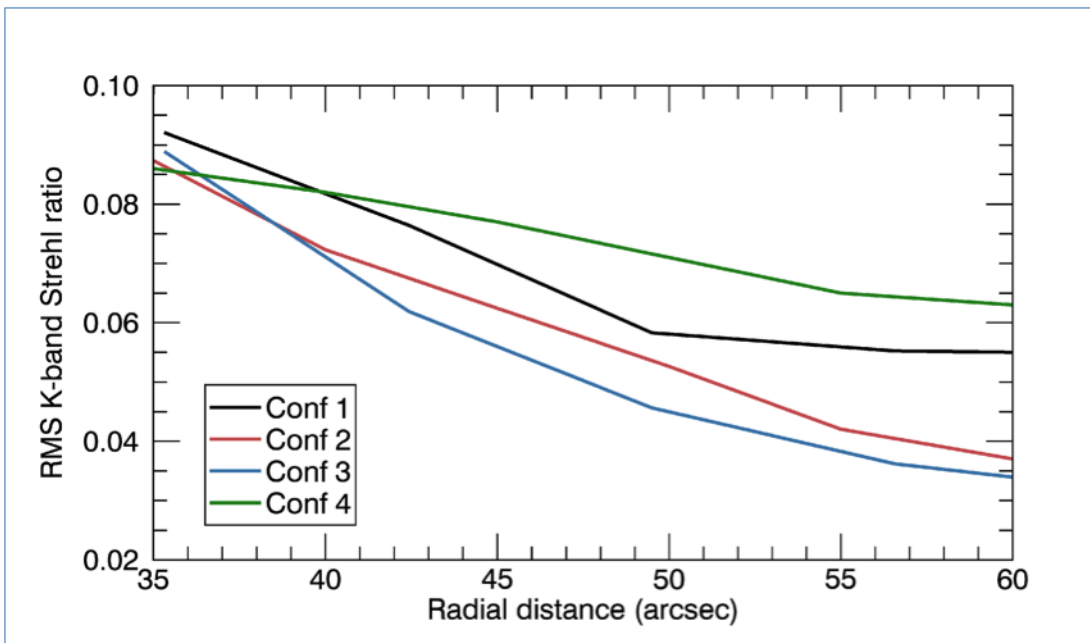


Figure 3. RMS associated to performance obtained in Figure 2

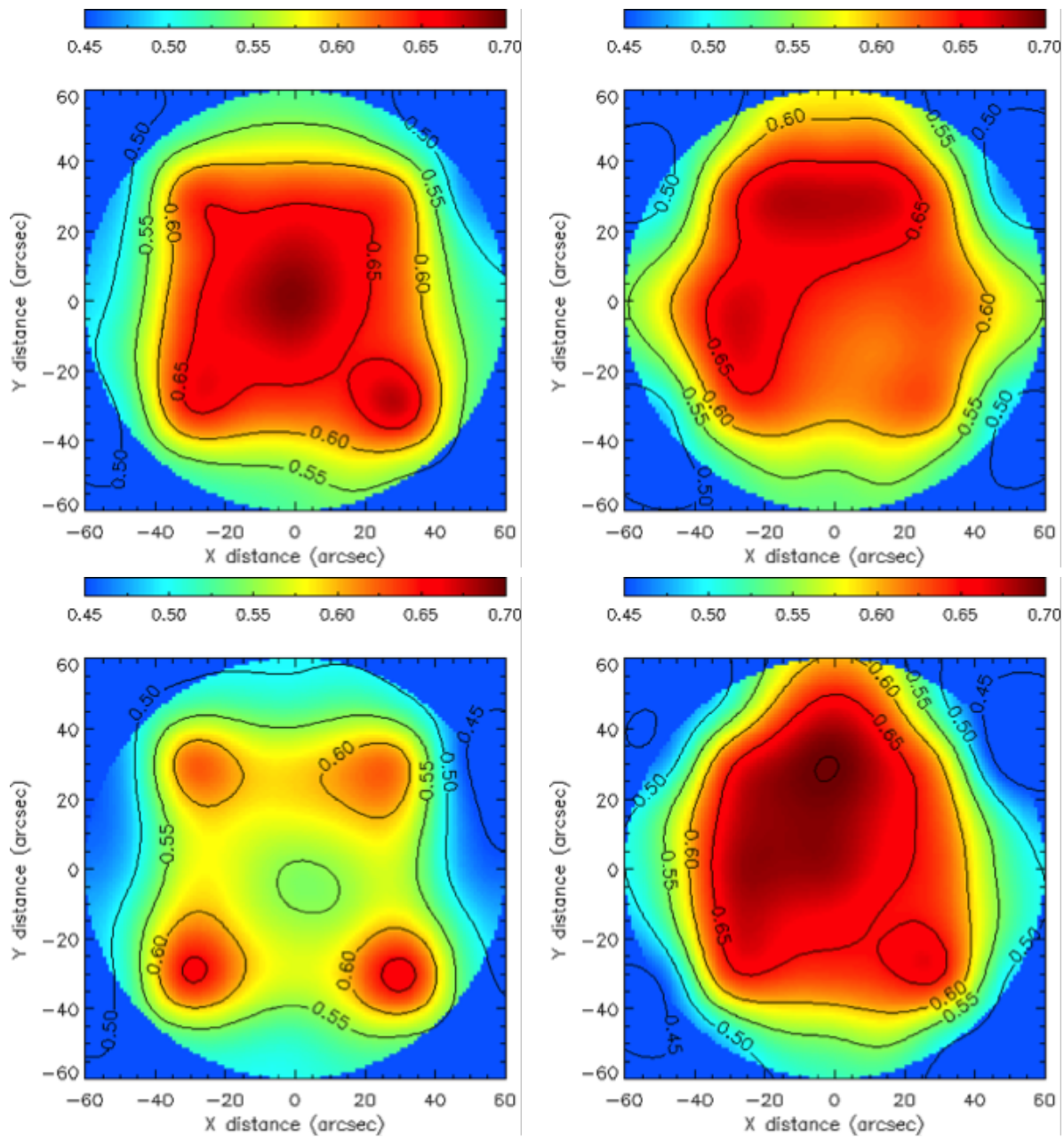


Table 4. Variation in K-band Strehl ratio across the field at zenith for Configurations 1, 2, 3 and 4 (from top left to bottom right). The radial distance in all cases was 50.

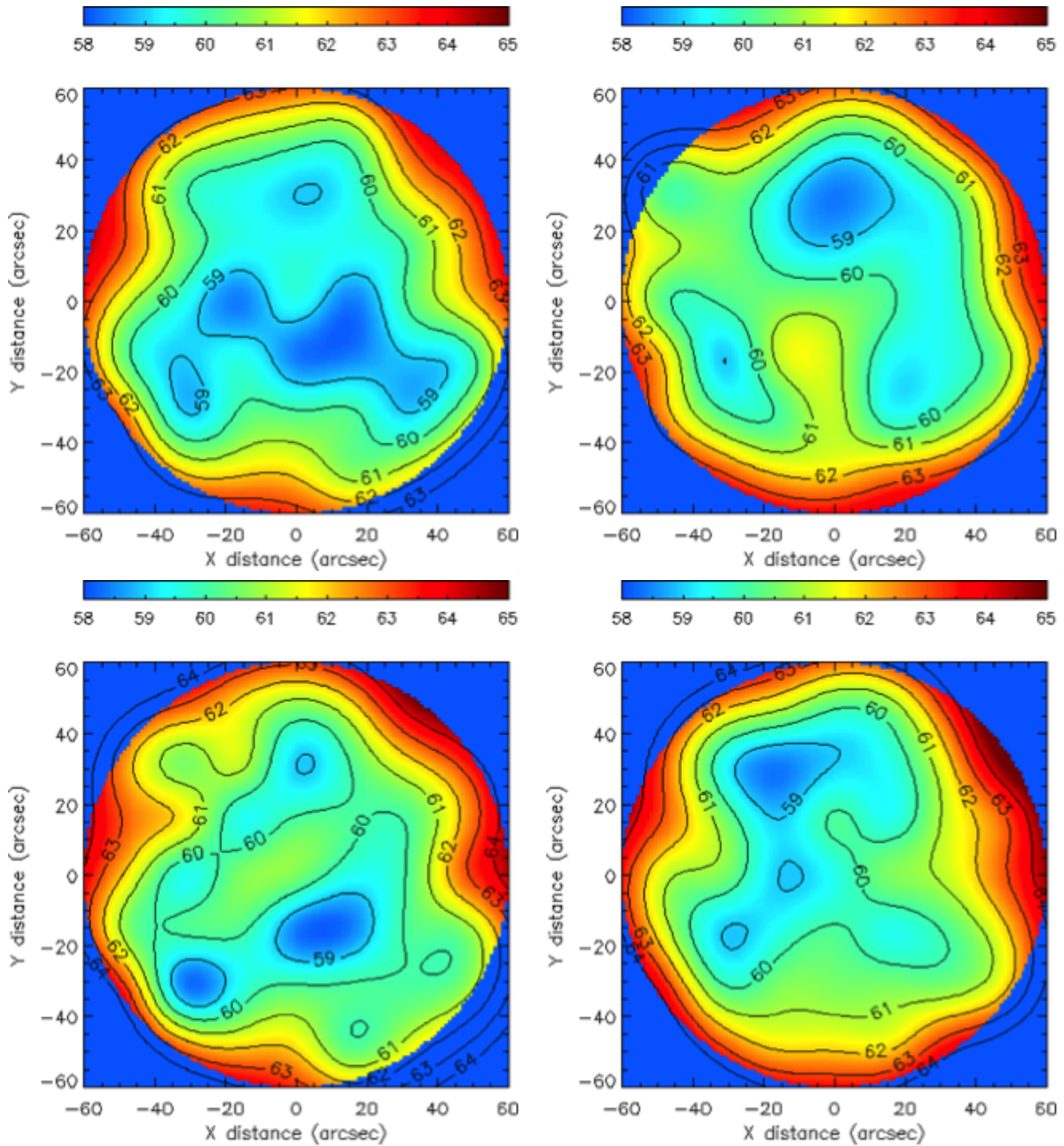


Table 5. Variation in K-band Strehl ratio across the field at zenith for Configurations 1, 2, 3 and 4 (from top left to bottom right). The radial distance in all cases was 50.

## 4.4 New baseline design

Since the conference (June 2019), we have advanced our design and we are now considering since first light the use of 5 laser guide stars most likely using 2 Toptica lasers one split in 2 and one split in 3. We also would like based on our simulation results to use 3 deformable mirrors to increase the uniformity and improved the generalized fitting error that is one of the main error term. These results and trades were presented at our conceptual design review in September 2019 and we are now preparing different call for proposals (different subsystems) to enter into the preliminary design phase.

## 5. CONCLUSION

As part of the National Science Foundation funded Gemini in the Era of Multi-Messenger Astronomy (GEMMA) program, Gemini Observatory is developing GNAO, a wide field adaptive optics (AO) facility for Gemini-North on Maunakea. GNAO will provide the user community with a queue-operated Multi-Conjugate AO (MCAO) system, enabling a wide range of innovative solar system, Galactic, and extragalactic science with a particular focus on synergies with JWST in the area of time-domain astronomy. The GNAO effort builds on institutional investment and experience with the more limited block-scheduled Gemini Multi-Conjugate System (GeMS), in operation at Gemini South since 2013.

The modular design of GNAO allows the observatory clear upgrade paths to not only better the GNAO system as proposed here but also to add new capabilities such as an Adaptive Secondary Mirror (ASM) and Ground Layer AO (GLAO) in the future enabling the observatory to quickly adapt capabilities in the era of multi-messenger astronomy.

The proposed baseline of GNAO is to provide a laser guide star facility of 5 LGSs coming from 2 toptica lasers, an adaptive optics bench with 3 deformable mirrors planes, 5 LGS WFSs and a focal plane WFS to TT sensing and plate scale corrections, a system controller and a real time computer facility. The proposed design of these systems will be presented later on this year (2020).

## ACKNOWLEDGMENTS

Based on observations obtained at the Gemini Observatory, which is operated by the Association of Universities for Research in Astronomy, Inc., under a cooperative agreement with the NSF on behalf of the Gemini partnership: the National Science Foundation (United States), National Research Council (Canada), CONICYT (Chile), Ministerio de Ciencia, Tecnología e Innovación Productiva (Argentina), Ministério da Ciência, Tecnologia e Inovação (Brazil), and Korea Astronomy and Space Science Institute (Republic of Korea). Gemini Observatory thanks the National Science Foundation for the GEMMA award.

## REFERENCES

- [1] Sivanandam, S., Chapman, S., Simard, L., Hickson, P., Venn, K., Thibault, S., Sawicki, M., Muzzin, A., Erickson, D., Abraham, R., Akiyama, M., Andersen, D., Bradley, C., Carlberg, R., Chen, S., Correia, C., Davidge, T., Ellison, S., El-Sankary, K., Fahlman, G., Lamb, M., Lardi ere, O., Lemoine-Busserolle, M., Moon, D.-S., Murray, N., Peck, A., Shafai, C., Sivo, G., Veran, J.-P., and Yee, H., “Gemini infrared multi-object spectrograph: instrument overview,” in [*Proc. SPIE*], *Society of Photo-Optical Instrumentation Engineers (SPIE) Conference Series* **10702**, 107021J (Jul 2018).
- [2] Sivo, G., Blakeslee, J., Lotz, J., Roe, H., Andersen, M., Scharwachter, J., Palmer, D., Kleinman, S., Adamson, A., Hirst, P., Marin, E., Catala, L., van Dam, M., Goodsell, S., Provost, N., Diaz, R., Jorgensen, I., Kim, H., Lemoine-Busserolle, M., Blain, C., Chun, M., Ammons, M., Christou, J., Bond, C., Sivanandam, S., Turri, P., Wizinowich, P., Correia, C., Neichel, B., Veran, J.-P., Esposito, S., Lamb, M., Fusco, T., Rigaut, F., and Steinbring, E., “Entering into the Wide Field Adaptive Optics Era on Maunakea,” *arXiv e-prints*, arXiv:1907.08169 (Jul 2019).

- [3] Rigaut, F., Neichel, B., Boccas, M., d’Orgeville, C., Vidal, F., van Dam, M. A., Arriagada, G., Fesquet, V., Galvez, R. L., Gausachs, G., Cavedoni, C., Ebberts, A. W., Karcwicz, S., James, E., Lührs, J., Montes, V., Perez, G., Rambold, W. N., Rojas, R., Walker, S., Bec, M., Trancho, G., Sheehan, M., Irarrazaval, B., Boyer, C., Ellerbroek, B. L., Flicker, R., Gratadour, D., Garcia-Rissmann, A., and Daruich, F., “Gemini multiconjugate adaptive optics system review - I. Design, trade-offs and integration,” *MNRAS* **437**, 2361–2375 (Jan. 2014).
- [4] Neichel, B., Rigaut, F., Vidal, F., van Dam, M. A., Garrel, V., Carrasco, E. R., Pessev, P., Winge, C., Boccas, M., d’Orgeville, C., Arriagada, G., Serio, A., Fesquet, V., Rambold, W. N., Lührs, J., Moreno, C., Gausachs, G., Galvez, R. L., Montes, V., Vucina, T. B., Marin, E., Urrutia, C., Lopez, A., Diggs, S. J., Marchant, C., Ebberts, A. W., Trujillo, C., Bec, M., Trancho, G., McGregor, P., Young, P. J., Colazo, F., and Edwards, M. L., “Gemini multiconjugate adaptive optics system review - II. Commissioning, operation and overall performance,” *MNRAS* **440**, 1002–1019 (May 2014).